



7th International Conference on Silicon Photovoltaics, SiliconPV 2017

Influence of temperature and residence time on thermal decomposition of monosilane

Guro M. Wyller^{*}, Thomas J. Preston, Trygve T. Mongstad, Dag Lindholm, Hallgeir Klette, Ørnulf Nordseth, Werner O. Filtvedt and Erik S. Marstein

Department of Solar Energy, Institute for Energy Technology (IFE), P.O. Box 40, NO-2027 Kjeller, Norway

Abstract

Thermal decomposition experiments with monosilane diluted in hydrogen have been conducted in a free-space reactor with an extendable reaction zone, allowing for easy variation of residence time. Reactor effluent was analyzed by gas-chromatography combined with mass-spectrometry (GC-MS). The applied analysis technique enables detection of silanes with up nine silicon atoms, as well as absolute quantification of the concentrations of mono-, di-, and trisilane. For all the detected silanes, our gas analyses show a peak in reactor outlet concentration as function of temperature whose position and shape depend on the number of silicon atoms (n_{Si}) contained in the silane species. The peak width decreases and the peak position shifts to higher temperatures with increasing n_{Si} . At increased residence time, the concentration peak shifts to lower temperatures and the SiH_4 consumption rate increases. This is consistent with the expected behavior for a system described by Arrhenius kinetics. The maximum outlet concentrations of all the measured silanes decrease with increasing residence time. However, the dependence of silane concentrations on temperature and residence time is not trivial: At a fixed temperature the measured outlet concentrations will increase with increasing residence time in some temperature regions and decrease with residence time in other temperature regions. By mapping outlet concentrations as function of temperature and residence time we attempt to decouple the effect of these two parameters and to untangle their effect from that of reactor geometry and operation.

© 2017 The Authors. Published by Elsevier Ltd.

Peer review by the scientific conference committee of SiliconPV 2017 under responsibility of PSE AG.

Keywords: Silane pyrolysis; Reactor kinetics; GC-MS analysis; Higher order silanes

^{*} Corresponding author. Tel.: +47 63 80 60 00

E-mail address: guro.marie.wyller@ife.no

1. Introduction

Improvements of photovoltaic (PV) manufacturing processes can significantly reduce the overall costs of solar electricity and simultaneously increase the life-cycle climate benefits of PV power generation. Recent analyses [1] show that reducing the energy consumption for solar grade silicon production by 15–17 kWh/kg_{Si} is – in a CO₂ emission perspective – equivalent to a 1 % increase in the baseline efficiency for mono Si and multicrystalline (mc) Si PV modules. Replacing the traditional Siemens process by less energy intensive solar grade silicon refining routes such as the fluidized bed reactor (FBR) route, which is considered one of the most promising alternatives to Siemens process [2], is one way of reducing the energy consumption related to solar grade silicon production. However, FBR operation meets challenges due to formation of dust particles (fines) and to material contamination from fines and from the reactor walls [3–5]. Detailed understanding on the thermal decomposition process of monosilane (SiH₄), which is the preferred source of silicon in FBR, is crucial for overcoming these challenges. Fundamental understanding of the thermal decomposition of monosilane can also accelerate optimization of chemical vapor deposition processes for semiconductor applications [6] and production of other novel forms of Si, such as nanoparticles for use in Li-ion batteries [7].

Numerous studies have been conducted, both experimentally [8–16 and others] and by modelling [6,8,10,13,17–19 and others], in order to broaden the understanding of thermal decomposition of monosilane and its dependence on reaction parameters such as temperature, inlet concentrations and residence time. Works investigating thermal decomposition of disilane (Si₂H₆) [20–22] are also of relevance for understanding the thermal decomposition of monosilane. One possible reason for such a variety of contributions without consensus is the difficulty of distinguishing underlying physical chemistry from the effects of the various reactors and measurement techniques that are applied.

Thermal decomposition of monosilane has been studied at low pressures [e.g. 13,23,25], atmospheric pressures [e.g. 9,14,15,26] and elevated pressures [e.g. 12,16] in various types of reactors, with differing sizes, geometries, flow rates and heat sources and with different dilution gases, including argon [25,27], hydrogen [14,15], [9], helium [27] and nitrogen [9]. Gaseous reaction products have been measured by various techniques, including, among others, gas chromatography (GC) [9,12], infrared emission [16,28], laser absorption [16,28] laser-induced fluorescence [29] and different types of mass spectrometry (MS), including electron ionization (EI) combined with single quadrupole MS mass spectrometry (MS) [8,10,24,30] and vacuum ultraviolet (VUV) photoionization time-of-flight (TOF) MS [27,31,32]. A common theme among the applied gas measurement techniques is that they struggle to detect silicon hydride species with number of silicon atoms $n_{Si} > 5$ and to distinguish between isomers with identical number of silicon atoms. We have previously applied GC-MS (gas chromatography combined with mass spectrometry) for measuring silicon hydrides with up to five silicon atoms and to distinguish between isomers of tetrasilanes (iso-tetrasilane and n-tetrasilane) [14]. In this contribution, we apply GC-MS for measuring silicon hydrides with up to nine silicon atoms. With the ability to detect these large silicon hydrides at varied reactor parameters, including temperature and residence time, we start building a framework for unveiling the underlying physical chemistry.

2. Experimental

2.1. Thermal decomposition reactor

Our pyrolysis experiments were conducted in a free-space reactor (Fig. 1) equipped with a preheating zone and four reaction zones in which the temperature can be set individually. Each reaction zone has a water cooling coil and a resistive heating coil. By varying the number of heating coils that are turned on, the residence time can easily be changed without altering the gas flow and thus the flow pattern in the reactor to a large extent.

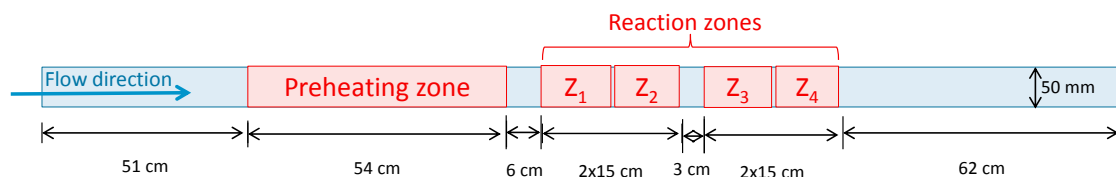


Fig. 1. The FSR used for the temperature residence time investigations is equipped with a 54 cm long preheating zone and four reaction zones, each with a length of 15 cm. The tube has an inner diameter of 50 mm and the walls are made of 3 mm thick 316-LN stainless steel.

For the experiments reported here we used a constant gas flow of 4.0 standard liters per minute (SLM), and monosilane inlet concentrations of 5.0 % and 10.0 %. H₂ was used as dilution gas and the reactor pressure was kept constant at 1 atm. The temperature in the active reaction zones was varied in the range 450 °C to 590 °C, whereas the temperature in the preheating zone was kept constant at 300 °C. Temperatures were measured at the reactor wall, as well as on a temperature probe placed in the reactor core. The probe is equipped with one thermocouple in the center of each reaction zone. In our measurements, the difference in absolute temperature between the wall and the reactor core is always less than 2.5%. In this contribution, all temperatures refer to the wall temperature. The temperature distribution and flow pattern within the reactor was estimated based on computational fluid dynamics (CFD) using the SiSim tool [33]. The model indicates large variations both in axial gas velocities and in temperature over the cross-section of the reactor. Therefore, defining the residence time corresponding to a certain number of active reaction zones is challenging. Table 1 lists low and high estimates for residence times with varying number of active heating zones. The low estimate defines residence time as the total time during which the CFD modelling reports the temperature for a gas parcel following the reactor center-line to be within 25°C of the set-point temperature. The high estimate defines residence time as the total time during which the CFD modelling reports the temperature for a gas parcel following a line 3.3 mm from the reactor wall to be within 25°C of the set-point temperature. In both definitions, because of slow heat transfer in the gas, the residence time in the case of only one reaction zone is 0 seconds. We do therefore not include data obtained with only one active reaction zone. Moreover, because of the large discrepancy between the low and the high estimates for residence time, we will in the following refer to number of active heating zones in our reactor rather than specifying a certain residence time. The large spread in actual residence times for gas parcels following different paths through the reactor leads to difficulties in separating fundamental chemistry from reactor physics, and addressing these issues is the theme of current work in our group.

Table 1. Low and high estimates for residence times resulting from various numbers of active reaction zones (see text).

Number of active reaction zones	Residence time (s)	
	Low estimate	High estimate
2 reaction zones	0.6	1.8
3 reaction zones	1.5	3.9
4 reaction zones	2.5	6.3

2.2. GC-MS measurement technique

The reactor exhaust was analyzed with an advanced combination of gas chromatography and mass spectrometry (GC Agilent 7890B combined with MS Agilent 5977A), already described briefly in a preceding contribution [13]. Saturated silanes are detected by an electron ionization (EI) quadrupole mass spectrometer (QMS). The electron energy was set to 70 eV. With the settings used, our GC-MS system gives the possibility for detection of silanes with up to nine silicon atoms. By choosing longer GC holding times, even higher order silanes can be detected. We use a selected ion monitoring (SIM) method, in which the ions for monitoring the higher order silanes were chosen based on the fragmentation patterns of full m/z scans of the smaller, more abundant silanes. Limiting the number of ions we monitor drastically improves the signal-to-noise-ratio for these higher order silanes. Fig. 2 shows the sum of the signal intensity for the selected ions as function of GC elution time as well as an assignment of the signals to groups of gas species.

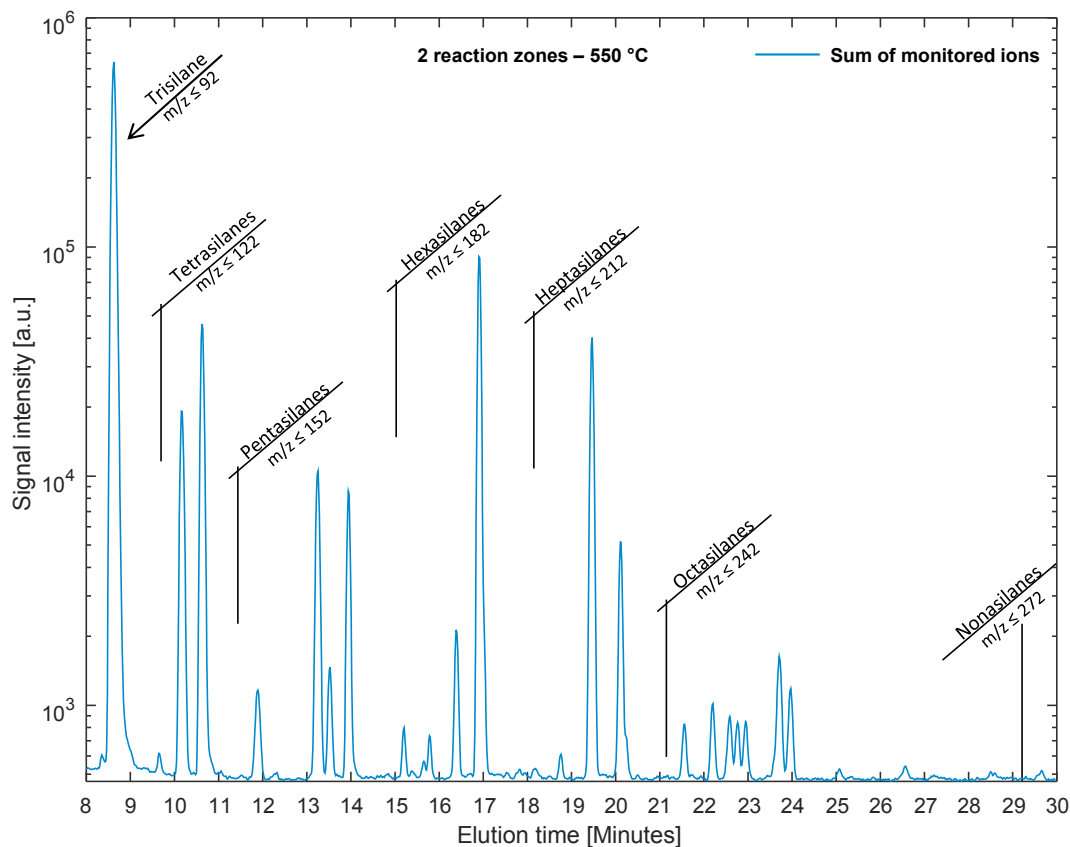


Fig. 2. Example ion chromatogram showing the sum of all monitored ions as function of GC retention time, for a reactor setting of two active reaction zones and a set temperature of 550 C. The monitored ions are $m/z = 60, 90, 116, 118, 120, 148, 150, 178, 180, 208, 210, 240$. The assignment of the peaks is based on mass spectral information (see text).

Assigning a GC peak to a specific silane species can be a challenge. For the purpose of this measurement, we use the highest m/z from our list of selected masses to assign each GC peak to a silane family (di-, tri-, tetra-, etc). The highest possible fragment masses for each silane family are indicated in Fig. 2. Within one silane family, assignment of GC peaks to specific isomers is aided by knowledge on boiling points and resulting GC retention times.

SiH_4 and Si_2H_6 were detected in a thermal conductivity detector (TCD) integrated in the GC setup. Three calibration standards (from Matheson) were used for obtaining absolute calibrations for SiH_4 , Si_2H_6 and Si_3H_8 . We are not yet able to calibrate the measurement signals for other silanes.

3. Results and discussion

3.1. Exhaust concentrations as function of temperature at various residence times

Fig. 3 shows exhaust concentrations of silanes with up to nine Si atoms as function of temperature, at two different residence time settings: two reaction zones (left column) and four reaction zones (right column). The upper panes display calibrated outlet concentrations for SiH_4 , Si_2H_6 and Si_3H_8 . The central panes show signal intensities in arbitrary units of all gas species measured by the mass spectrometer in our setup (silanes with $3 \leq n_{\text{Si}} \leq 9$). The bottom panes show the measured signal for each species normalized to the maximum signal for that species.

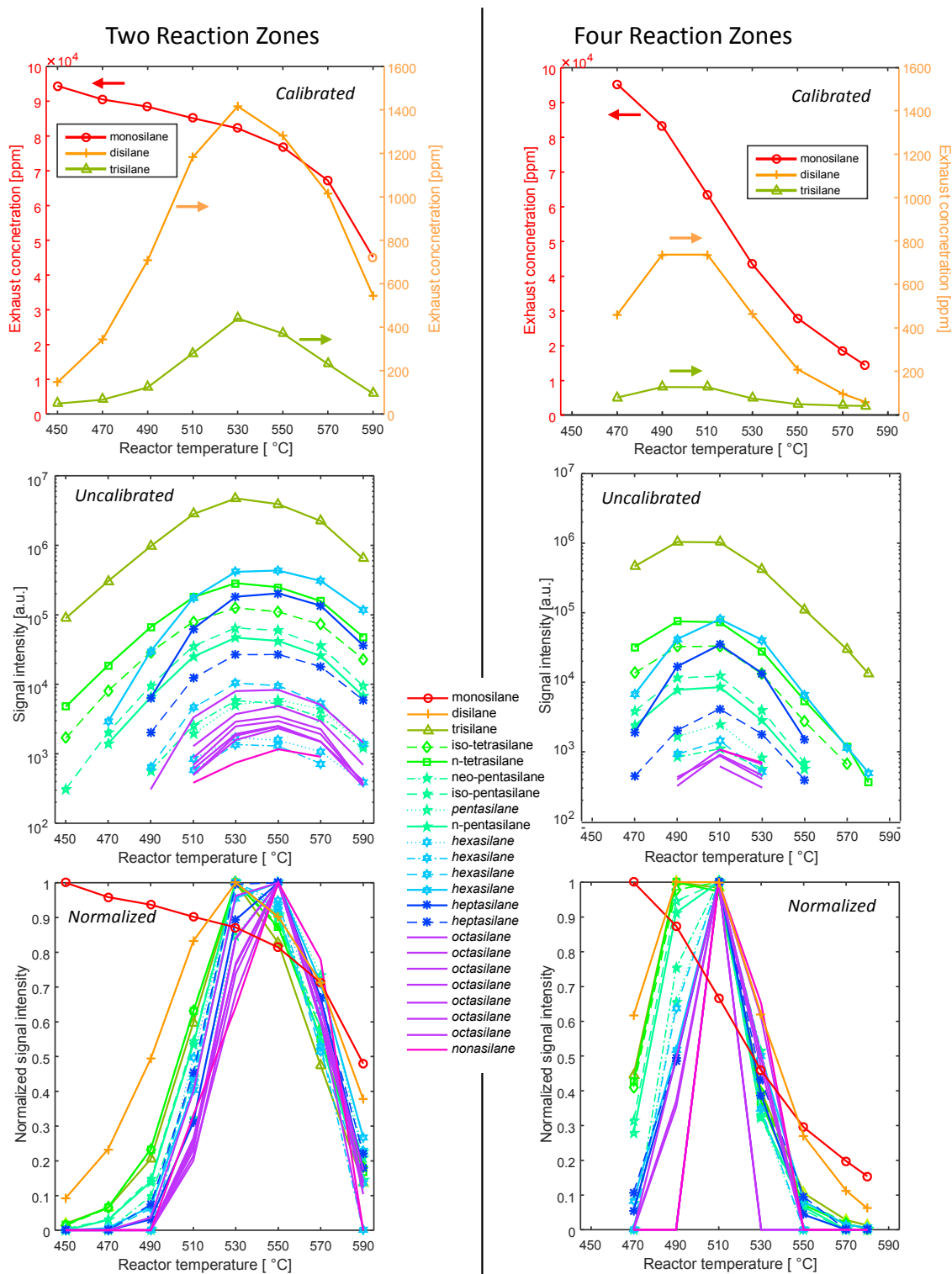


Fig. 3. Outlet concentration of silanes as function of temperature at two different residence time settings: two reaction zones (left column) and four reaction zones (right column) during thermal decomposition of SiH_4 diluted in H_2 . The inlet silane concentration $\text{SiH}_{4\text{inlet}}$ is 10%. Upper row: calibrated outlet concentrations for SiH_4 , Si_2H_6 and Si_3H_8 . Central row: signal intensities in arbitrary units for silanes with $3 \leq n_{\text{Si}} \leq 9$, as measured by mass spectrometry. Bottom row: measured signal for each species normalized to the maximum signal for that species.

As expected, the concentration of SiH_4 is close to $\text{SiH}_{4\text{inlet}} = 10\%$ at the lowest temperatures in both residence time settings (upper panes of Fig. 3), indicating that little decomposition takes place at temperatures below about 450°C . For both cases, the SiH_4 concentration steadily decreases with increasing temperature, indicating that an increasing amount of SiH_4 reacts and forms higher order silanes. Furthermore, the increase of residence time from 2 to 4 zones also substantially increases SiH_4 consumption as function of temperature, which is consistent with a system described by Arrhenius kinetics.

An increase in the exhaust concentration of all the measured gas species in a narrow temperature range is seen for both residence time cases, starting at about 480°C for two reaction zones and at about 470°C for four reaction zones. The build-up of gas-phase intermediates in a narrow temperature range during thermal decomposition of SiH_4 is known from literature for species with up to four silicon atoms [9,14,15,24,30]. Our results (Fig. 3, central and bottom panes) reveal that the peak in outlet concentrations for a certain temperature range is present for silanes with up to nine silicon atoms. Our results further indicate that the peak shifts to higher temperatures and becomes narrower with increasing number of silicon atoms contained in the species. Similar development of species concentrations as function of temperature and number of silicon atoms have previously been reported during thermal decomposition of disilane (Si_2H_6) diluted in argon [20], but has – to the best of our knowledge – not been observed for thermal decomposition of monosilane in hydrogen.

Comparison of the two residence time cases (Fig. 3, left and right) indicates that the maximum outlet concentration appears at lower temperatures when the residence time is increased. The increase in residence time obtained when increasing the number of heated zones from 2 to 4 gives a shift in peak position of approximately 30°C for Si_2H_6 . The temperature shift is similar for all the measured silanes. Other authors [8] have reported a peak in the concentration of Si_2H_6 whose position along the residence time dimension changed as function of temperature. As we will explain in section 3.2, our sketch of Si_2H_6 concentration as function of both temperature and residence time in Fig. 4 (right panel) illustrates that there is qualitative agreement between their results [8] and the findings we are presenting here.

The maximum absolute outlet concentration of all measured gas intermediates is considerably reduced when the residence time is increased by increasing the effective reactor length from two zones to four zones (Fig. 3, left and right). In the case of disilane, the maximum concentration is reduced from about 1400 ppm at the shorter residence time to about 700 ppm at the longer residence time. For the other measured silanes, the increase in residence time causes a reduction in maximum outlet concentration of about 70 % - 85 %. The decrease in maximum outlet concentrations at longer residence time indicates that as residence time increases a larger fraction of the silicon atoms contained in the initially injected SiH_4 has undergone reactions to form silicon hydrides with $n_{\text{Si}} \geq 9$ (not measured here), also including silicon particles. The subtleties of how the concentrations of the higher order silanes change with different reactor conditions present an excellent target for chemical modelling, the focus of forthcoming work from our group.

3.2. Combined influence of residence time and temperature on exhaust concentrations

Fig. 4 illustrates how the outlet gas concentrations are affected by variations in residence time by showing outlet concentration of disilane as a function of temperature at two different residence times (left panel) and as a function of residence times at three different temperatures (central panel). That is to say, the data presented in the left and central panes of Fig. 4 are two different representations of the same, just plotted along two orthogonal axes: temperature and time. Disilane is a stable intermediate between the starting material, monosilane, and the ending material, solid silicon. Its concentration in the reactor exhaust, therefore, results from a balance between all the reaction rates that produce disilane and all those rates that consume it. If we take an Arrhenius perspective of the chemical reaction rates,

$$r_i \propto e^{-E_{a,i}/RT}, \quad (1)$$

then the concentrations we measure are naturally variables of temperature T and time t via integration of the rate r_i . Here, $E_{a,i}$ is the activation energy of a particular reaction r_i , and R is the universal gas constant.

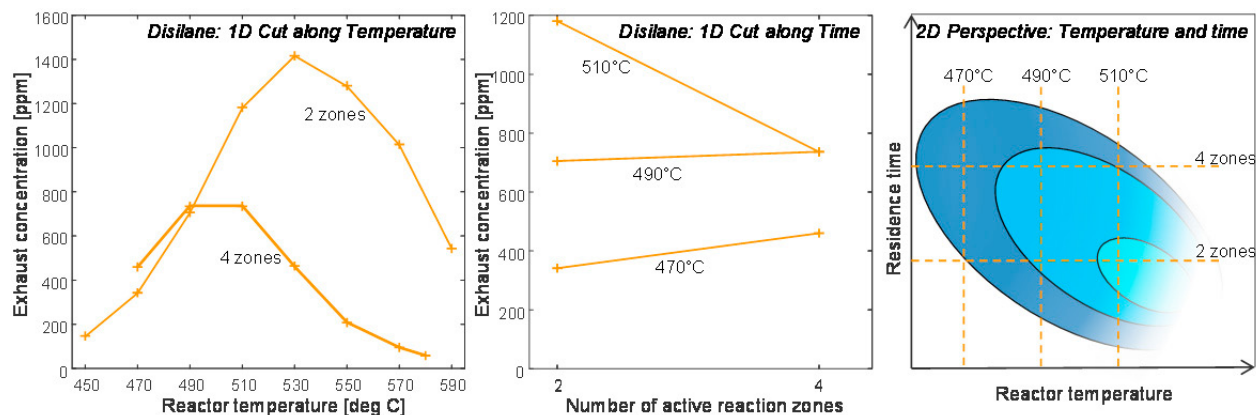


Fig. 4. Left: Outlet concentration of disilane as function of temperature at two different residence times. Central: Outlet concentration of disilane as function of temperature at three different temperatures. Right: Sketch of disilane concentration as a function of reactor temperature and residence time. The portion of the graph corresponding to short residence times and high temperatures is faded out to indicate that region of the landscape is, as yet, unexplored.

Although both increased temperature and longer residence times push the chemistry further through the reaction network, their effects on *concentration* of intermediates are different. Again, if we take an Arrhenius perspective of the *rate*, we expect this difference because the two variables appear in different ways: time from integration of the rate, and temperature from the rate itself. The curves shown in the left and central panes of Fig. 4, can be seen as parts of the surface describing outlet concentrations of disilane as functions of both reactor temperature and residence time. The shape of this surface, with decreasing peak temperature for longer residence times (left panel), lower maximum outlet concentration for longer residence times (left panel), and the appearance of both rising and falling concentrations with fixed temperature and increasing residence time (central panel) indicates the complexity of the dependence of the Si_2H_6 concentration on the two dimensions. The right panel of Fig. 4 shows a sketch of disilane concentration as a function of both temperature and residence time. The contour profiles are consistent with the measured data but are only to illustrate our point. While Fig. 4 only displays the concentration of disilane, the concentrations of other species show a similar pattern. The position of the global maximum and the gradient of the curve in both directions will differ depending on the species. The exact shape of such plots can, with further experimentation and modelling of the chemical reaction network, teach us about how to best control the chemistry that converts SiH_4 into solid silicon.

3.3. Changes in measured exhaust concentrations as function of reactor operation history

During our monosilane decomposition experiments, in which we scan the reactor temperature up and then down, we observed a slight hysteresis in the measured outlet concentrations of all the included silanes as function of temperature. The behavior of the hysteresis depends on reactor temperature and residence time as well as on number of silicon atoms in the measured silane species. The magnitude of the hysteresis does not affect the conclusions of the current work. Rather, the nuance allowed by our new measurement technique will allow us to ask more detailed questions in the future. Present experiments and current understanding make it difficult to know the source of this hysteresis, but we attempt to name some possibilities here.

Because of the high boiling points of large silicon hydrides, they can condense in the transmission line between the reactor and the GC-MS, which is held at a temperature of about 60 °C. Phase transition equilibrium reactions between condensed silanes in the transmission line and the reactor effluent flowing through the line will cause changes to the composition of the measured reactor effluent. The boiling points for SiH_4 , Si_2H_6 and Si_3H_8 are all below the boiling temperature of the transmission line [34]. However, trapping of these light silanes in heavier silicon hydrides might give raise to a hysteresis effect also for the lighter species.

During reactor operation, aerosol particles and wall deposits are being formed. Accumulation of particles with a porous surface structure can significantly increase the available surface area and thus the rates of heterogeneous

reactions. Reactor flow pattern and temperature distribution may also be altered by particle depositions. It is therefore not unlikely that the observed hysteresis effect is a result of particles building up in the reactor. Onischuk et al. [30] have earlier reported a dependence of reactor effluent composition on reactor operation time, and attributed the effect to accumulation of particles with a porous surface structure.

4. Conclusion

Our investigations of thermal decomposition of monosilane with varied temperature and residence time indicate that the maximum outlet concentrations of silicon hydrides shift to lower temperatures when the residence time is increased. The peak in outlet concentration as function of temperature, as well as its shift with residence time, is measured for silicon hydrides with up to nine silicon atoms. At one fixed residence time, the peak width decreases and the peak position shifts to higher temperatures with increasing number of silicon atoms contained in a silane species.

Within the range of residence times that we have investigated, the maximum outlet concentration of silanes decreases with increasing residence time. However, as both temperature and residence time influence the concentration of gas intermediates, the measured outlet concentrations at a fixed temperature will increase with increasing residence time in some temperature regions and decrease with residence time in other temperature regions.

In an Arrhenius perspective, the exhaust concentration of each silane is a function both of temperature via the rates of all reactions in which each silane is produced and consumed, and of residence time via the integration of these rates. Theoretically decoupling the effects of the two dimensions is challenging. Our investigation is a starting point to empirically map outlet concentrations of the higher silanes as surfaces in the three dimensional space of temperature, residence time and concentration. Knowing the shape of these surfaces – which is different for each species in the reaction network – can, with further experimentation and modelling of the chemical reaction network, teach us about how to best control the chemistry that converts SiH_4 into solid silicon. With this perspective in hand, the PV community can reap the benefits from continued improvement in the silicon-production process.

Acknowledgements

The authors would like to thank the Norwegian Research Council for funding through The Norwegian Research Centre for Solar Cell Technology (NFR project no. 193829/E20). We are also grateful for discussions with Stein Julsrud and Edgar Estupi an at REC Silicon, Moses Lake, US.

References

- [1] Ravikumar D, Wender B, Seager TP, Fraser MP, Tao M. A climate rationale for research and development on photovoltaics manufacture. *Appl Energy* 2017;189:245–56.
- [2] Bye G, Ceccaroli B. Solar grade silicon: Technology status and industrial trends. *Sol Energy Mater Sol Cells* 2014;130:634–46.
- [3] Ramos A, Filtvedt WO, Lindholm D, Ramachandran PA, Rodr guez A, del Ca izo C. Deposition reactors for solar grade silicon: A comparative thermal analysis of a Siemens reactor and a fluidized bed reactor. *J Cryst Growth* 2015;431:1–9.
- [4] Li J, Chen G, Zhang P, Wang W, Duan J. Technical challenges and progress in fluidized bed chemical vapor deposition of polysilicon. *Chinese J Chem Eng* 2011;19:747–53.
- [5] Filtvedt WO, Holt A, Ramachandran PA, Melaaen MC. Chemical vapor deposition of silicon from silane : Review of growth mechanisms and modeling / scaleup of fluidized bed reactors. *Sol Energy Mater Sol Cells* 2012;107:188–200.
- [6] Slakman BL, Simka HS, Reddy H, West RH. Extending Reaction Mechanism Generator (RMG) to silicon hydride chemistry. *Ind Eng Chem Res* 2016;acs.iecr.6b02402.
- [7] Mangolini L. Synthesis, properties, and applications of silicon nanocrystals 2013;31:1–29.
- [8] Onischuk AA, Levykin AI, Strunin VP, Ushakova MA, Samoilova RI, Sabelfeld KK, et al. Aerosol formation under heterogeneous/homogeneous thermal decomposition of silane: Experiment and numerical modelling. *J Aerosol Sci* 2000;31:879–906.
- [9] Slootman F, Parent J-C. Homogeneous gas-phase nucleation in silane pyrolysis. *J Aerosol Sci* 1994;25:15–21.
- [10] Onischuk AA, Strunin VP, Ushakova MA, Panfilov VN. Studying of silane thermal decomposition mechanism. *Int J Chem Kinet* 1998;30:99–110.
- [11] Odden JO, Halvorsen G, Rong H, Gl ckner R. Comparison of the energy consumption in different production processes for solar grade silicon. *Silicon Chem Sol Ind* 2008;9:16.

- [12] Odden JO, Egeberg PK, Kjekshus A. From monosilane to crystalline silicon, Part I: Decomposition of monosilane at 690–830K and initial pressures 0.1–6.6MPa in a free-space reactor. *Sol Energy Mater Sol Cells* 2005;86:165–76.
- [13] Nijhawan S, McMurry PH, Swihart MT, Suh S-M, Girshick SL, Campbell SA, et al. An experimental and numerical study of particle nucleation and growth during low-pressure thermal decomposition of silane. *J Aerosol Sci* 2003;34:691–711.
- [14] Wyller GM, Preston T, Mongstad TT, Klette H, Nordseth  , Lindholm D, et al. Thermal Decomposition of Monosilane observed in a Free Space Reactor. *EU PVSEC XXXII 2BO.2.2*, Munich: 2016, p. 294–9.
- [15] Wyller GM, Preston TJ, Klette H, Nordseth  , Mongstad T, Filtvedt WO, et al. Critical Nucleation Concentration for Monosilane as Function of Temperature Observed in a Free Space Reactor. *Energy Procedia* 2016;92:904–12.
- [16] Petersen EL, Crofton MW. Measurements of High-Temperature Silane Pyrolysis Using SiH₄ IR Emission and SiH₂ Laser Absorption. *J Phys Chem A* 2003;107:10988–95.
- [17] Swihart MT, Girshick SL. Thermochemistry and Kinetics of Silicon Hydride Cluster Formation during Thermal Decomposition of Silane. *J Phys Chem B* 1999;103:64–76.
- [18] Dang HY, Swihart MT. Computational Modeling of Silicon Nanoparticle Synthesis: I. A General Two-Dimensional Model. *Aerosol Sci Technol* 2009;43:250–63.
- [19] Menz WJ, Kraft M. A new model for silicon nanoparticle synthesis. *Combust Flame* 2013;160:947–58.
- [20] Tonokura K, Murasaki T, Koshi M. Formation Mechanism of Hydrogenated Silicon Clusters during Thermal Decomposition of Disilane. *J Phys Chem B* 2002;106:555–63.
- [21] Yoshida K, Matsumoto K, Oguchi T, Tonokura K, Koshi M. Thermal decomposition mechanism of disilane. *J Phys Chem A* 2006;110:4726–31.
- [22] Tonokura K, Murasaki T, Koshi M. Diagnostics of the gas-phase thermal decomposition of Si₂H₆ using vacuum ultraviolet photoionization. *Chem Phys Lett* 2000:507–11.
- [23] Qian ZM, Michiel H, Van Ammel A, Nijs J, Mertens R, Interuniversitair. Homogeneous Gas Phase Nucleation of Silane in Low Pressure Chemical Vapor Deposition (LPCVD). *J Electrochem Soc SOLID-STATE Sci Technol* 1988;135:2378–9.
- [24] Simon J, Feurer R, Reynes A, Morancho R. Thermal dissociation of disilane : quadrupole spectrometry investigation 1992;24:51–9.
- [25] Onischuk A., Levykin A., Strunin V., Sabelfeld K., Panfilov V. Aggregate formation under homogeneous silane thermal decomposition. *J Aerosol Sci* 2000;31:1263–81.
- [26] Eversteijn FC. Gas-phase Decomposition of silane in a horizontal epitaxial reactor. *Philips Res Repts* 1971;26:134–44.
- [27] Chambreau SD, Zhang J. VUV photoionization time-of-flight mass spectrometry of flash pyrolysis of silane and disilane. *Chem Phys Lett* 2001;343:482–8.
- [28] Knights JC. High resolution absorption and emission spectroscopy of a silane plasma in the 1800–2300 cm⁻¹ range. *J Chem Phys* 1982;76:3414.
- [29] Ho P, Coltrin ME, Breiland WG. Laser-Induced Fluorescence Measurements and Kinetic Analysis of Si Atom Formation in a Rotating Disk Chemical Vapor Deposition Reactor. *J Phys Chem* 1994;98:10138–47.
- [30] Onischuk AA, Strunin VP, Ushakova MA, Panfilov VN. On the pathways of aerosol formation by thermal decomposition of silane. *J Aerosol Sci* 1997;28:207–22.
- [31] Tonokura K, Koshi M. Reaction kinetics in silicon chemical vapor deposition. *Solid State Mater Sci* 2002;6:479–85.
- [32] Duan HL, Zaharias GA, Bent SF. Probing radicals in hot wire decomposition of silane using single photon ionization. *Appl Phys Lett* 2001;78:1784–6.
- [33] Mortensen D, Lindholm D, Friestad K, Henriksen BR, Fj er HG, Rudshaug M, et al. Crystallization furnace modeling including coupled heat and fluid flow, stresses and deformations. *Energy Procedia* 2013;38:597–603.
- [34] Hidding B. Untersuchung der Eignung von Silanen als Treibstoffe in der Luft- und Raumfahrt 2004:1–176.